Symmetry-aware Texture Refinement for 3D Building Models via Massing Decomposition and Generative AI

Fan Xue[1,*], Yijie Wu[2], Maosu Li[3]

[1] The University of Hong Kong, Pokfulam, Hong Kong (China SAR) - xuef@hku.hk
[2] Hong Kong Polytechnic University, Hunghom, Hong Kong (China SAR) - yijie.wu@polyu.edu.hk
[3] Hong Kong University of Science and Technology (Guangzhou), Guangdong, China – maosuli@hkust-gz.edu.cn

Keywords: Mesh texture, Massing decomposition, 3D building model, Generative AI, Symmetry.

Abstract

Three-dimensional (3D) building models with accurate geometry and realistic textures remain essential for city information modeling and digital twin applications. However, photogrammetric reconstructions consistently suffer from severe texture defects caused by occlusions, shadows, distortions, and projection errors. Existing approaches either rely on rigorous photometric optimization that demands topological correctness and multi-view imagery, or employ flexible AI-driven generation that leverages semantics but often lacks geometric constraints. This paper presents a novel hybrid framework that exploits architectural regularities—specifically massing decomposition and partial symmetries—to guide high-fidelity texture refinement. We first decompose building meshes into mass-aligned convex volumes using MorphCut. Textures are then reprojected onto these volumes, followed by Building Section Skeletons to pair symmetric facades and establish precise geometric correspondences. Finally, generative AI is applied using symmetry-aware constraints to achieve contextually accurate inpainting and correction. Pilot studies on three Hong Kong buildings demonstrate robust decomposition, faithful texture transfer, and effective defect mitigation, while revealing current limitations of unconstrained generative models in preserving floor counts and structural regularity. The proposed symmetry-guided pipeline notably advances the reliable and semantically coherent reconstruction of textures for complex urban buildings.

1. Introduction

1.1 Background

Three-dimensional (3D) building models with accurate geometry, realistic texture, and rich semantics are fundamental to city information modeling (CIM) (Kamra et al., 2022; Xue et al., 2021). The 3D building models and CIM subsequently support modern urban planning, digital twin development, and immersive simulation environments (Biljecki et al., 2015; Li et al., 2026; Meng et al., 2026). Modern photogrammetry and LiDAR methods have made notable advancements in this domain (Jiang et al., 2021; Xue et al., 2021).

However, a primary challenge in all methods is the unsatisfactory texture quality of buildings, particularly for those with complex geometry. Such texture defects can arise from data acquisition, including occlusions, heavy shadows, distortions, and missing images. They can also result from reconstruction pipelines, such as geometric mesh errors, vertex misalignments, clutter disruptions, and projection errors across multiple images.

1.2 Existing methods

Texture refinement of 3D building models has been addressed in many studies. Broadly, there are two categories: photometric optimization and AI-driven generation. Photometric optimization mainly relies on classical photogrammetric principles. These methods iteratively adjust the input mesh, including its geometry, to minimize photometric errors between the geometry and the source data. One example is Rothermel et al. (2020), who adapted the texture consistency of photographs from high-resolution multi-view satellite imagery to refine geometric details. Iwaszczuk and Stilla (2017) focused on line-based matching and camera pose refinement to process thermal infrared images for uncertain 3D models with image sequences.

The second category is AI-driven generation, which applies modern deep learning, particularly diffusion models and Generative Adversarial Networks (GANs), to synthesize, repair, and enhance textures (Buyukdemircioglu et al., 2022). Diffusion models learn to reverse a gradual noising process and have proven effective for upsampling low-quality textures and inpainting missing regions for 3D texture refinement. One example is Elevate3D, which balanced quality and fidelity through variable noise handling (Ryu et al., 2025). Another example is TwinTex, which used a fine-tuned diffusion model to inpaint missing regions on abstracted building models (Xiong et al., 2023). GANs can translate semantic label mappings into photorealistic images. For instance, Shang et al. (2023) repaired texture defects using facade semantics such as “window”, “wall”, and “door”, along with architectural style images.

In general, photometric optimization methods are stringent about data inputs, including a coarse mesh model and multiple views of imagery, and rely less on semantics. The topological correctness of the coarse mesh enables iterative geometric and texture optimization. In contrast, AI-driven generation methods are more flexible in terms of data inputs but closely relate to building semantics, whether explicitly or implicitly. Some studies hybridized processes from both categories to take advantage of both topology (and geometry) and semantics for 3D building models. For example, Texture2LoD3 integrated ray-casting, image rectification, semantic segmentation, and data fusion to combine low-detail semantic building models (e.g., LoD1 or LoD2 CityGML) with geo-referenced panoramic street-level im-

* Corresponding author

This is the author's version of the paper:
Xue, F., Wu, Y., & Li, M. (2026). Symmetry-aware Texture Refinement for 3D Building Models via Massing Decomposition and Generative AI. *ISPRS Archives of the Photogrammetry, Remote Sensing and Spatial Information Sciences*. (accepted, in press). DOI: <to be confirmed>

agery (Tang et al., 2025). The AI components were particularly effective in isolating facade regions and removing cars, pedestrians, and vegetation from textures.

1.3 Motivation

Architectural regularities include lines, planes, volumes, symmetries, and their combinations. Such regularities serve as ubiquitous and natural guides in texture refinement, particularly within photometric optimization. Examples are the line matching for uncertain 3D models in Iwaszczuk and Stilla (2017) and planar consistency for texture defragmentation in Liu et al. (2024). A recent advance for regular architectural volumes is the Building Section Skeletons (BSS) method, which pairs internal and partial symmetric facades (Wu et al., 2024). Based on the BSS, MorphCut decomposes convex volumes of building massing to align with architectural structures (Wu et al., 2025). These developments in processing regular lines and planes, particularly symmetric massing volumes, motivate this study and serve as its foundational preprocessing.

Another motive arises from emerging applications of generative AI (GenAI). GenAI can synthesize novel, photorealistic texture data to overcome data defects. It can inpaint missing regions, upscale blurry images to high fidelity, and generate contextually accurate details (e.g., windows and doors) from semantic prompts and guides. Even plausible "hallucinations" of entirely missing textures can supplement information creatively to produce complete, detailed, and visually consistent 3D building models.

2. Research Methods

The methods presented in this paper aim to leverage building symmetry and massing decomposition, as well as GenAI, for texture inpainting and correction of 3D building models. There are three steps, with one more preprocessing step. Section 2.1 emphasizes the preparatory step of decomposing building models into mass-aligned volumetric components. Section 2.2 details how to reproject photogrammetric textures onto the volumes. Section 2.3 pairs the symmetric skeletons and the projected textures. The final refinement step in Section 2.4 utilizes GenAI for high-fidelity, context-aware error mitigation.

2.1 Preprocessing of 3D building model decomposition by MorphCut

The preprocessing step involves segmenting the 3D building model into mass-aligned parts that capture the volumetric and semantic structure of architectural designs. Building mass is defined as the aggregate form composed of distinct elements, such as podiums and towers. The building mass serves as a critical prior for texture analysis, as it correlates with material and stylistic consistency within components while allowing for variation across them.

Then, we employ MorphCut in (Wu et al., 2025) to decompose an input building into mass-aligned parts. The input is a 3D building model represented as a triangle mesh. MorphCut first processes the model by reconstructing its geometry, eliminating topological errors, and ensuring a watertight manifold surface.

The core of MorphCut's approach is a best-first branch-and-bound (BBnB) procedure (Land and Doig, 2009), enhanced with key morphological characteristics of buildings. The BBnB algorithm decomposes the building model into as few convex or near-convex parts as possible, ensuring that the resulting segments align closely with the building's underlying massing structure through the integration of architectural morphology.

2.2 Step 1: Texture reprojection

After the decomposition, textures from the original photogrammetric mesh are reprojected onto the external facets of the decomposed parts. The resulting grouped textures serve as priors for subsequent texture refinement using GenAI.

We then implement this via a straightforward reprojection procedure. First, the decomposed model and the original photogrammetric mesh are aligned at their centroids and base elevations. Their orientations remain consistent, as MorphCut's reconstruction preserves the original model's orientation.

Next, rays are emitted from the external faces of the decomposed model along their respective face normals to intersect the photogrammetric mesh. Upon intersection, each ray retrieves color information from the corresponding location on the photogrammetric surface and transfers it back to the originating face. A higher sampling density on the external faces results in higher-resolution textures but typically incurs greater computational cost.

2.3 Step 2: Pairing BSS construction and texture

The final phase involves constructing BSS within each decomposed part and pairing symmetric facades to quantify texture inconsistencies, thus establishing geometric constraints for GenAI-based refinement. BSS, conceptualized as medial sheets approximating midpoints between parallel surfaces, extends traditional skeletonization techniques to architectural contexts, capturing partial symmetries reflecting common design regularities.

For each decomposed part, we use ODAS (Xue et al., 2019) to detect its primary vertical symmetry plane. ODAS formulates symmetry detection as a derivative-free optimization problem. With 1,000 iterations, it reliably produces precise symmetry planes with low root-mean-square deviation (RMSD). This detected plane serves as the primary symmetry plane for the part. Additionally, we compute a secondary vertical symmetry plane orthogonal to the primary one, as many convex building components exhibit cuboid-like geometry, possessing two orthogonal pairs of symmetric facades.

Once the primary and secondary symmetry planes are determined for each part, the faces parallel to these planes are projected orthogonally onto the respective symmetry planes to delineate their vertical extents. Since all parts are convex or near-convex, the resulting projection outlines are typically simple. For computational efficiency and simplicity, we approximate these outlines as rectangles. This allows us to pair the textures on opposing faces parallel to each symmetry plane. Consequently, each symmetry plane is associated with a corresponding pair of textures, which guide symmetry-aware texture refinement in subsequent GenAI processing.

2.4 Step 3: Texture refinement

The texture refinement first applies shadow removal to the reprojected paired textures, followed by cross-image harmonization to improve the illumination consistency between symmetric facade pairs. Both steps operate in the CIE LAB color space.

The shadow removal corrects anomalously dark rows by a multiplicative per-row gain on the L channel with concurrent A and B color cast correction. The harmonization then unifies the L profiles of the paired textures toward their element-wise maximum and shifts the A and B channels toward their grand mean to correct white balance discrepancies.

We further select representative reprojected textures from each decomposed part to evaluate the performance of GenAI and vision-language models (VLMs) in refining building textures. The format of prompts to VLM in this paper is as follows: "[Standard texture repair prompts] + [geometric guidelines from BSS-texture mapping] + [special notes for certain (e.g., high-rise facade) tasks]." This pilot study aims to inform the development of future AI-powered workflows for high-fidelity, context-aware texture refinement in 3D architectural models. Therefore, the prompt format is relatively simple for clarity and reproducibility.

3. Experimental Results

3.1 Experimental settings

The proposed method was evaluated through pilot studies on three buildings in Hong Kong, as shown in Figure 1. The three test cases represent low-rise, mid-rise, and high-rise building structures from 3D building models and the iB1000 topographical map from the Common Spatial Data Infrastructure of Hong Kong (Available at: https://portal.csdi.gov.hk); the cases include one school and two residential buildings. Figure 1 illustrates the 2D footprints and the 3D realistic meshes for these cases. The selected buildings exhibit clear massing structures and high symmetry. Notably, Case 2 is situated in a relatively dense environment, where textures may be incomplete or distorted due to limited scanning angles and occlusions. Case 3 is exceptionally tall and surrounded by other high-rise structures, which results in heavy shadowing on the textures.

3.2 Results of Step 1

Figure 2 shows the building convex decomposition, the corresponding BSS, and the reprojected textured parts for the three cases. The MorphCut method successfully decomposed the original meshes into compact, mass-aligned convex parts that preserve the geometric integrity of the buildings. The extracted BSS captured the dominant structural symmetry and alignment directions, particularly the two principal vertical symmetric planes in each case, demonstrating the robustness of the extraction process even for complex multi-tower configurations. The reprojected textured parts further confirm the accuracy of the decomposition and reprojection steps, as the textures remain well aligned with the facades and roofs of the original photogrammetric meshes, maintaining visual realism and architectural consistency across the reconstructed models.

3.3 Results of Step 2

Paired textures are shown for two decomposed parts in Case 1. 'Pos' and 'Neg' denote the positive and negative symmetric sides of each part, respectively. The textures on the left correspond to the blue part in Figure 2, while those on the right correspond to the red part. Some facets on the symmetric planes lie inside the building; therefore, no textures are projected onto them.

Figure 3 presents two pairs of symmetric textures from Case 1. As the building is located in a relatively open environment, the reprojected textures show generally good quality, with only minor shadow effects. Although the two symmetric planes display different visual appearances due to lighting and viewpoint variations, their geometric structures, including the number of floors and floor heights, remain consistent, confirming the accuracy of the symmetry detection and texture projection.

More pronounced issues appear in the paired textures of Cases 2 and 3, primarily due to their more complex geometries and surrounding environments (Figure 4). In Case 2, noticeable texture distortions occur because the building is in close proximity to neighboring structures, which obstruct certain viewing angles during image acquisition. In Case 3, heavy shadows are cast on the main facades as the tall building is surrounded by other high-rise structures, leading to strong shadowing effects and slight texture distortions near the lower facades.

3.4 Results of Step 3

The visual consistency between each paired texture is quantified by the Structural Similarity Index Measure (SSIM) and the Root Mean Square Deviation (RMSD) of the Gaussian-smoothed L, a, and b channel maps. The SSIM is calculated by comparing local patterns of pixel intensities normalized for luminance and contrast to assess structural alignment, while the deviations, denoted as $RMSD_L$, $RMSD_a$, and $RMSD_b$, are derived by suppressing high-frequency structural content to isolate the low-frequency illumination field.

Three pairs of facade textures were selected for evaluation. Figure 5 presents the refinement results, and the corresponding quantitative metrics are summarized in Table 1. The refinement process improves brightness and color uniformity, which leads to an increase in SSIM as the removal of inconsistent lighting allows the underlying structural similarities of the symmetric facade pairs to be more accurately captured. Conversely, the RMSD of the smoothed L, a, and b values consistently decreases across all tested pairs, confirming that the procedure effectively suppresses heavy shadows and reduces brightness discrepancies between symmetric facades.

To evaluate the performance of GenAI and VLMs in texture refinement, we tested two scenarios: refining a single texture and refining a symmetric pair of textures. For both scenarios, we compared the outputs of two VLMs, ChatGPT 5 and Gemini, using carefully crafted prompts that emphasized visual quality and structural consistency. For the single texture refinement (Figure 6a), the prompt instructed the model to remove the heavy shadow from the facade texture. Both ChatGPT and Gemini produced refined results with improved luminance and reduced shadow artifacts, though differences in contrast handling and detail preservation are observable between the two models. For the symmetric pair refinement (Figure 6b), the prompt instructed the models to remove the heavy shadow from the facade texture, harmonize the luminance between the two facade textures, and output the refined results side by side. However, both VLMs failed to remove the heavy shadow effectively. ChatGPT partially addressed the issue by improving the overall brightness, yet the shadow remained prominent. Gemini, on the other hand, notably altered the visual appearance of one of the textures, compromising its structural and perceptual consistency with the original.

These results indicate that current VLMs, without fine-tuning and careful conditioning implementation, cannot properly handle

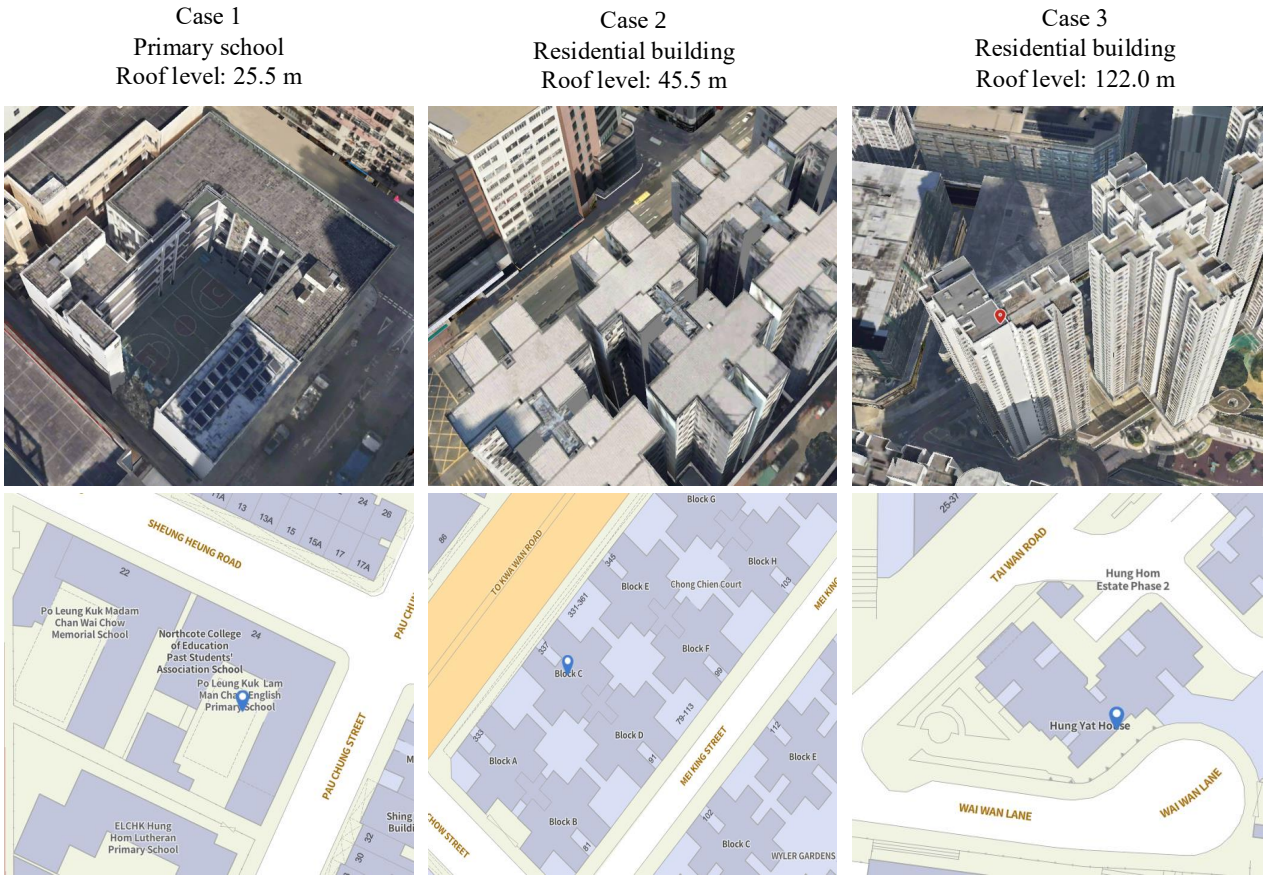

Figure 1. Three test cases of building models in this paper.

Table 1. Visual consistency between paired facade textures before and after the illumination refinement procedure. The arrows in the column headers indicate the direction of higher visual consistency.

	SSIM ↑		$RMSD_L$ ↓		$RMSD_a$ ↓		$RMSD_b$ ↓	
	Before	After (Δ)	Before	After (Δ)	Before	After (Δ)	Before	After (Δ)
Paired texture 1	**0.2673**	0.1666 (−0.1007)	0.2453	**0.1901** (−0.0552)	0.0230	**0.0119** (−0.0110)	0.0470	**0.0264** (−0.0205)
Paired texture 2	**0.2232**	0.2008 (−0.0224)	0.2906	**0.1320** (−0.1586)	0.0230	**0.0092** (−0.0138)	0.0624	**0.0233** (−0.0392)
Paired texture 3	**0.2634**	0.2008 (−0.0626)	0.2958	**0.1376** (−0.1581)	0.0222	**0.0097** (−0.0125)	0.0446	**0.0251** (−0.0194)

cross-texture refinement and consistency. This highlights the need for more targeted model adaptation strategies to achieve perceptually consistent and structurally faithful facade texture refinement across paired inputs.

4. Conclusion and Further Research

This study proposes a symmetry-aware and GenAI-supported framework for the refinement of 3D building textures. The method integrates mass-aligned decomposition, texture reprojection, and the pairing of symmetric facades through Building Section Skeletons (BSS). The experimental results across low-rise, mid-rise, and high-rise buildings demonstrate that the approach preserves geometric integrity, enhances texture alignment, and captures structural symmetry even in complex environments. The findings confirm that architectural regularities, when combined with generative capabilities, can improve texture completeness and visual realism. The work also highlights the potential of combining classical photogrammetric principles with modern AI models for high-fidelity, context-aware texture refinement.

However, several limitations remain in the paper, despite promising results. First, the framework relies on accurate mass decomposition and reliable symmetry detection, which may be compromised by highly irregular geometries or non-orthogonal photogrammetric meshes, such as heritage structures common in European or Asian historic cores. Secondly, pre-trained general-purpose GenAI models can introduce structural inconsistencies, particularly when generating textures for high-rise facades with repeated patterns. The current prompting strategy is simple and not fully optimized for architectural constraints. Last but not least, there were too few test cases and insufficient benchmarks and metrics in this preliminary study on integrating building mass symmetry with GenAI.

Accordingly, future research can incorporate explicit geometry-preserving priors, multi-view constraints, and adaptive prompts informed by building semantics. Integrating physics-based rendering cues, photometric-semantics integrations (Wu et al., 2026), and training task-specific generative models may also improve structural fidelity. Expanding the evaluation to more diverse building types, such as those in European cities (Wysocki et al., 2026), and large-scale urban scenes will further validate the

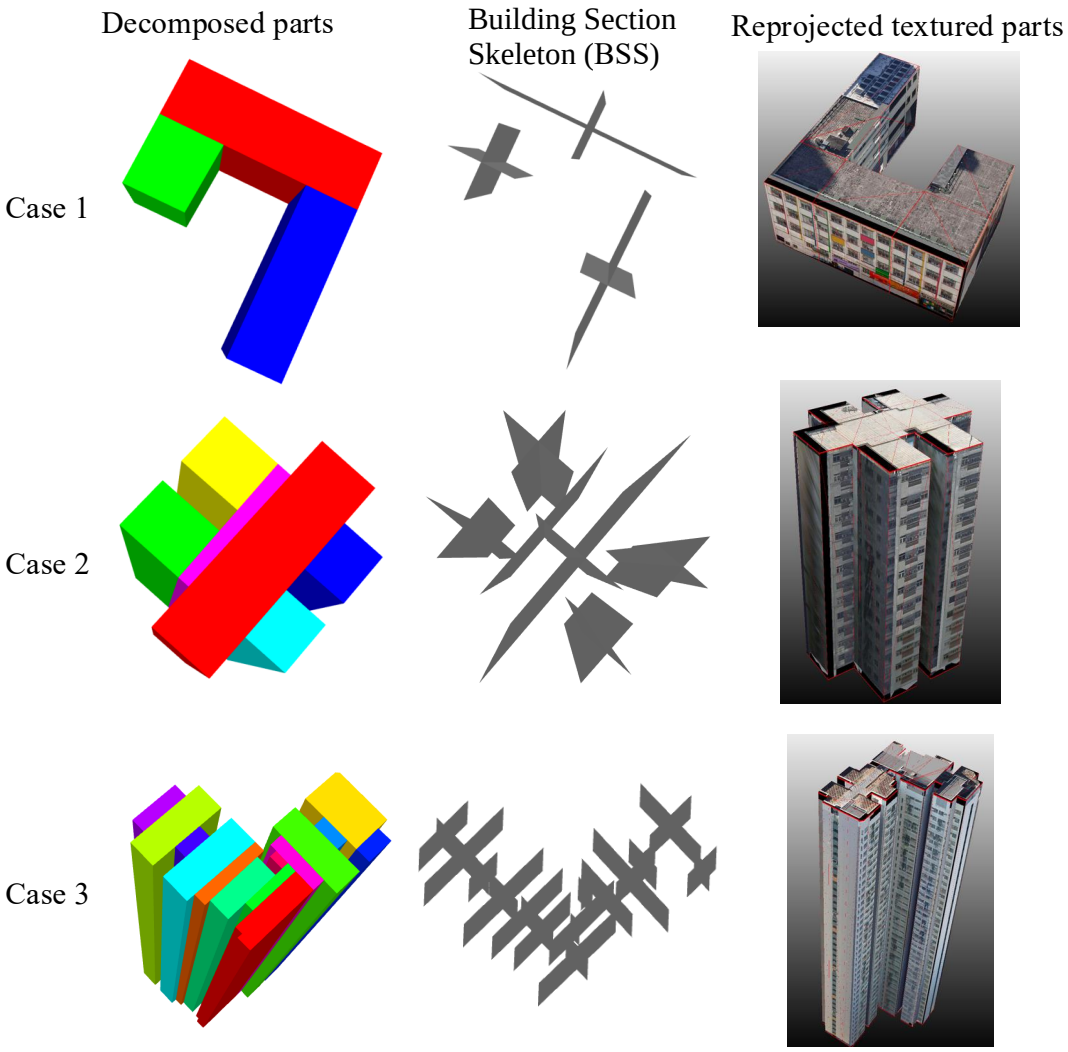

Figure 2. Decomposed parts, BSS, and reprojected textured parts of three test cases.

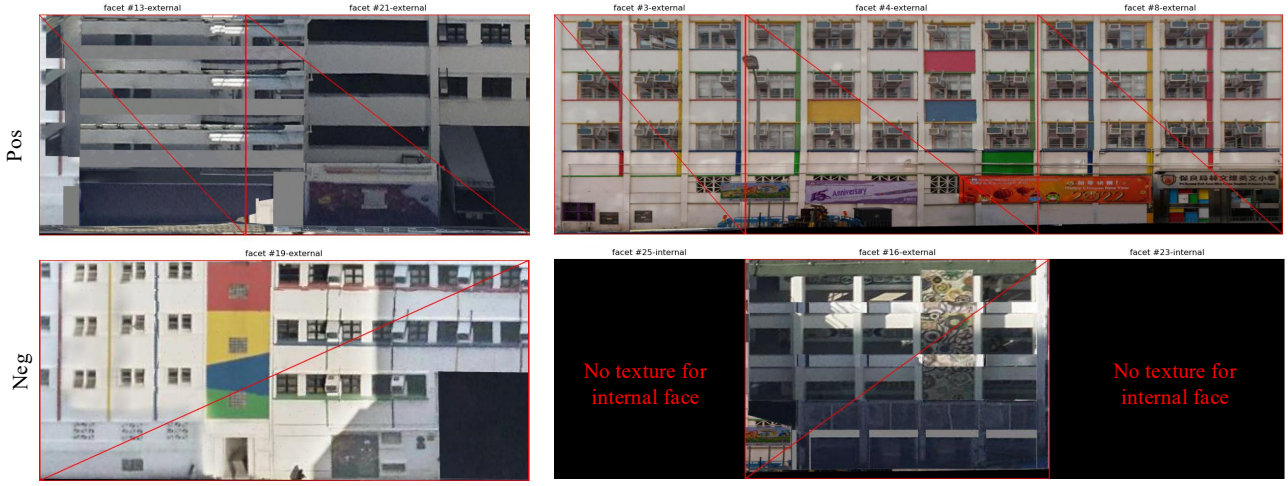

Figure 3. Paired textures for two decomposed parts in Case 1. Note: 'Pos' and 'Neg' denote the positive and negative symmetric sides of each part, respectively. The textures on the left correspond to the blue part shown in Figure 2, while those on the right correspond to the red part. Note that some facets on the symmetric planes are located internally within the building, and therefore no textures are projected onto them.

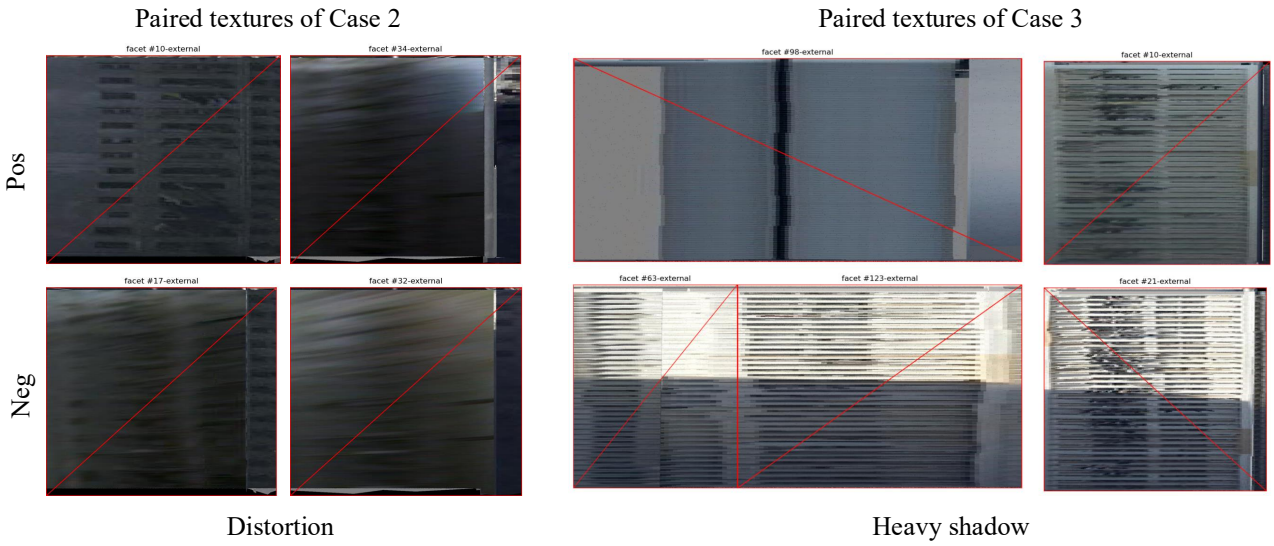

Figure 4. Distortion and heavy shadows observed in the projected textures of Cases 2 and 3.

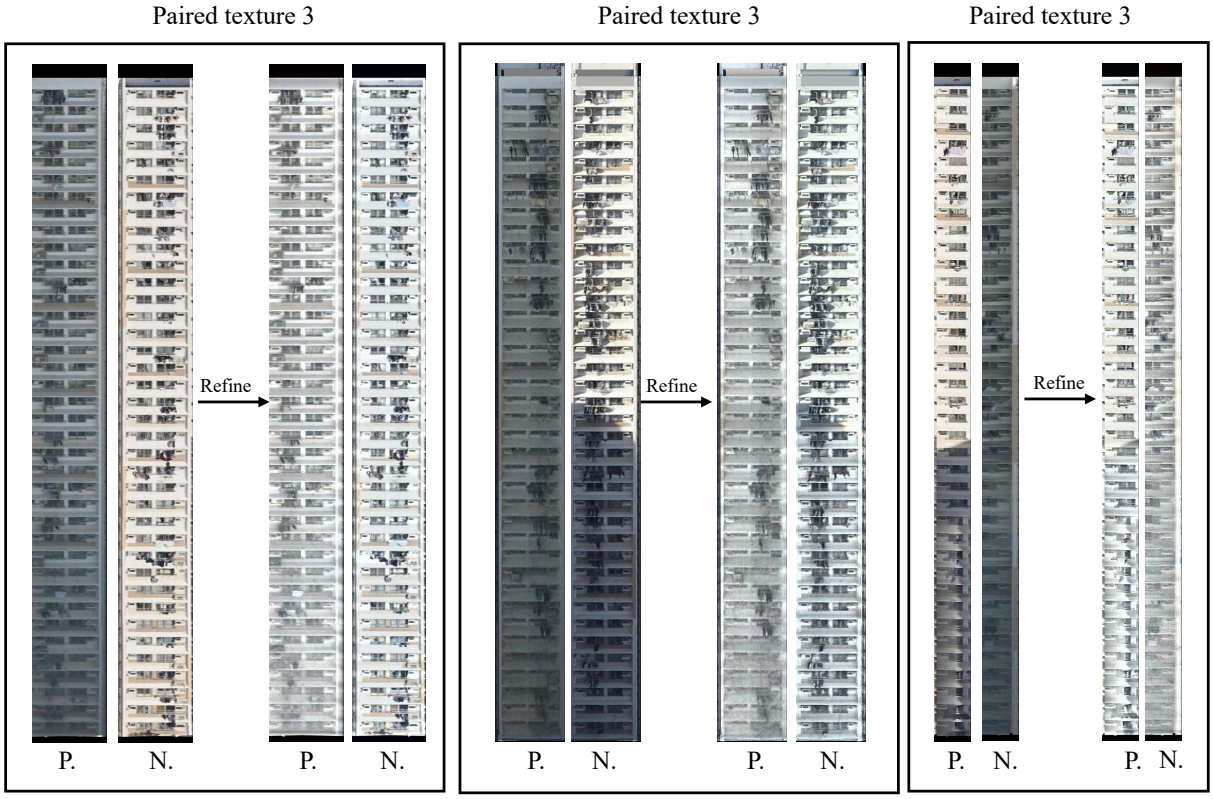

Figure 5. Paired textures before and after illumination refinement for three decomposed parts of Case 3. For each part, the positive (P.) and negative (N.) symmetric facade textures are shown before (left) and after (right) the refinement procedure, demonstrating the reduction in shadow and color temperature discrepancies between symmetric pairs.

robustness and generalizability of the proposed workflow.

Acknowledgment

The work presented in this paper was supported by the Hong Kong Research Grants Council (RGC) (No. 17201325) and the Department of Science and Technology of Guangdong Province (GDST) (2023A1515010757).

References

Biljecki, F., Stoter, J., Ledoux, H., Zlatanova, S., Çöltekin, A., 2015. Applications of 3D city models: State of the art review. *ISPRS International Journal of Geo-Information*, 4(4), 2842–2889. https://doi.org/10.3390/ijgi4042842.

Buyukdemircioglu, M., Kocaman, S., Kada, M., 2022. Deep learning for 3D building reconstruction: A review.

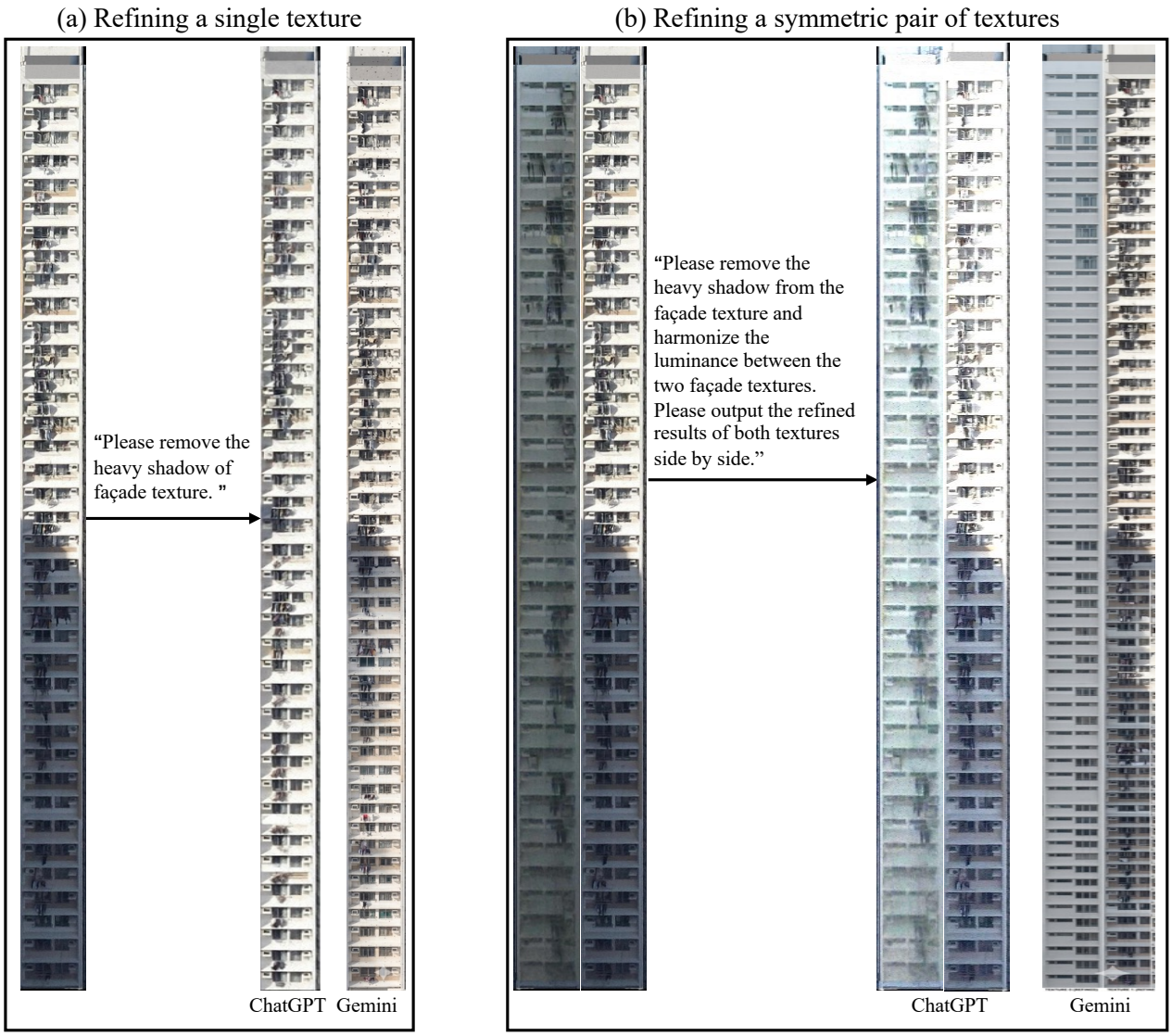

Figure 6. Texture refinement using VLM (models: ChatGPT 5 and Gemini).

International Archives of the Photogrammetry, Remote Sensing and Spatial Information Sciences, 43, 359–366. https://doi.org/10.5194/isprs-archives-XLIII-B2-2022-359-2022.

Iwaszczuk, D., Stilla, U., 2017. Camera pose refinement by matching uncertain 3D building models with thermal infrared image sequences for high quality texture extraction. *ISPRS Journal of Photogrammetry and Remote Sensing*, 132, 33–47. https://doi.org/10.1016/j.isprsjprs.2017.08.006.

Jiang, S., Jiang, W., Wang, L., 2021. Unmanned Aerial Vehicle-Based Photogrammetric 3D Mapping: A survey of techniques, applications, and challenges. *IEEE Geoscience and Remote Sensing Magazine*, 10(2), 135–171. https://doi.org/10.1109/MGRS.2021.3122248.

Kamra, V., Kudeshia, P., ArabiNaree, S., Chen, D., Akiyama, Y., Peethambaran, J., 2022. Lightweight reconstruction of urban buildings: Data structures, algorithms, and future directions. *IEEE Journal of Selected Topics in Applied Earth Observations and Remote Sensing*, 16, 902–917. https://doi.org/10.1109/JSTARS.2022.3232758.

Land, A. H., Doig, A. G., 2009. An automatic method for solving discrete programming problems. *50 Years of Integer Programming 1958-2008: From the Early Years to the State-of-the-Art*, Springer, 105–132.

Li, M., Guo, S., Duarte, F., Kumar, A., Kobori, N., Xue, F., Zhuang, W., Yeh, A. G., Ratti, C., 2026. Influence of objective and perceived exposures to urban nature on people's happiness. *npj Urban Sustainability*, 6, 6. https://doi.org/10.1038/s42949-025-00306-9.

Liu, B., Liu, W., Lei, Z., Zhang, F., Huang, X., Awwad, T. M., 2024. A Planar Feature-Preserving Texture Defragmentation Method for 3D Urban Building Models. *Remote Sensing*, 16(22), 4154. https://doi.org/10.3390/rs16224154.

Meng, S., Wu, L., Li, M., Yeh, A. G., Xue, F., 2026. Automated window detection for digital twin buildings: A generalized 'sandwich' model and practical guidelines. *Energy and Buildings*, 360, 117384. https://doi.org/10.1016/j.enbuild.2026.117384.

Rothermel, M., Gong, K., Fritsch, D., Schindler, K., Haala, N., 2020. Photometric multi-view mesh refine-

ment for high-resolution satellite images. *ISPRS Journal of Photogrammetry and Remote Sensing*, 166, 52–62. https://doi.org/10.1016/j.isprsjprs.2020.05.001.

Ryu, N., Won, J., Son, J., Gong, M., Lee, J.-H., Cho, S., 2025. Elevating 3D models: High-quality texture and geometry refinement from a low-quality model. *Proceedings of the Special Interest Group on Computer Graphics and Interactive Techniques Conference Conference Papers*, 165, 1–12.

Shang, Q., Hu, H., Yu, H., Xu, B., Wang, L., Zhu, Q., 2023. Semantic Image Translation for Repairing the Texture Defects of Building Models. *IEEE Transactions on Geoscience and Remote Sensing*, 62, 1–20. https://doi.org/10.1109/TGRS.2023.3338962.

Tang, W., Li, W., Liang, X., Wysocki, O., Biljecki, F., Holst, C., Jutzi, B., 2025. Texture2LoD3: Enabling LoD3 building reconstruction with panoramic images. *Proceedings of the Computer Vision and Pattern Recognition Conference*, 2016–2026.

Wu, X., Yang, T., Yu, L., Cao, J., Si, H., 2026. Efficient semantic-aware texture optimization for 3D scene reconstruction. *Computers & Graphics*, 134, 104529. https://doi.org/10.1016/j.cag.2025.104529.

Wu, Y., Xue, F., Li, M., Chen, S.-H., 2024. A novel Building Section Skeleton for compact 3D reconstruction from point clouds: A study of high-density urban scenes. *ISPRS Journal of Photogrammetry and Remote Sensing*, 209, 85–100. https://doi.org/10.1016/j.isprsjprs.2024.01.020.

Wu, Y., Xue, F., Nan, L., Wu, L., Stoter, J., Yeh, A. G., 2025. MorphCut: an efficient convex decomposition method of 3D building models for urban morphological analytics. *International Journal of Geographical Information Science*, 1–23. https://doi.org/10.1080/13658816.2025.2562251.

Wysocki, O., Schwab, B., Biswanath, M. K., Greza, M., Zhang, Q., Zhu, J., Froech, T., Heeramaglore, M., Hijazi, I., Kanna, K. et al., 2026. TUM2TWIN: Introducing the large-scale multimodal urban digital twin benchmark dataset. *ISPRS Journal of Photogrammetry and Remote Sensing*, 232, 810–830. https://doi.org/10.1016/j.isprsjprs.2025.12.013.

Xiong, W., Zhang, H., Peng, B., Hu, Z., Wu, Y., Guo, J., Huang, H., 2023. Twintex: Geometry-aware texture generation for abstracted 3D architectural models. *ACM Transactions on Graphics*, 42(6), 1–14. https://doi.org/10.1145/3618328.

Xue, F., Lu, W., Webster, C. J., Chen, K., 2019. A derivative-free optimization-based approach for detecting architectural symmetries from 3D point clouds. *ISPRS Journal of Photogrammetry and Remote Sensing*, 148, 32–40. https://doi.org/10.1016/j.isprsjprs.2018.12.005.

Xue, F., Wu, L., Lu, W., 2021. Semantic enrichment of building and city information models: A ten-year review. *Advanced Engineering Informatics*, 47, 101245. https://doi.org/10.1016/j.aei.2020.101245.